# Enhanced removal of antibiotics in hospital wastewater by Fe-ZnO activated persulfate oxidation

G.N. Coulibaly, S. Bae, J. Kim, A.A. Assadi, K. Hanna

# Enhanced removal of antibiotics in hospital wastewater by Fe-ZnO activated persulfate oxidation

Gnougon Nina COULIBALY[1,2], Sungjun BAE[2], Joohyun KIM[2], Aymen Amin ASSADI[1], Khalil HANNA[1*]

[1]Univ. Rennes, Ecole Nationale Supérieure de Chimie de Rennes, CNRS, ISCR-UMR 6226, F-35000 Rennes, France

[2]Department of Civil and Environmental Engineering, Konkuk University, 120 Neungdong-ro, Gwangjin-gu, Seoul 05029, Republic of Korea

*Corresponding author: khalil.hanna@ensc-rennes.fr

## Graphical Abstract

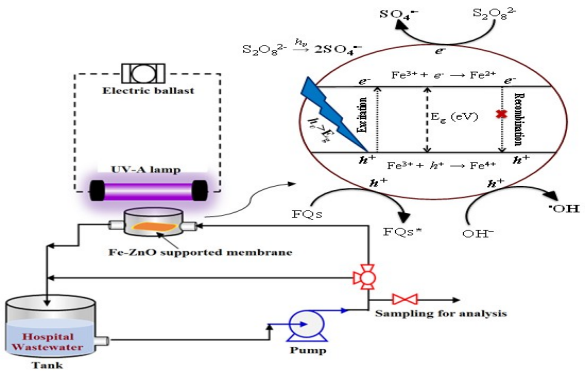


A recirculation reactor system using Fe-doped zinc oxide supported membrane and UVA irradiation was designed to remove fluoroquinolones in hospital wastewaters.

**Abstract**

Removal of two widely used antibiotics, flumequine (FLU) and ciprofloxacin (CIP), in synthetic and real hospital wastewaters was investigated using Fe-doped zinc oxide (Fe-ZnO) and UVA irradiation. The Fe-ZnO was supported on cellulose acetate membrane and integrated in a recirculation reactor system, designed for continuous oxidative treatment of contaminated wastewaters. Addition of low concentration of persulfate (e.g. 0.5 mM) improved considerably the degradation extent, where sulfate radicals were found to be the most involved oxidizing species. Oxidation rate constants decreased in mixture systems with respect to those of individual compounds, because of competition effects with radical species. Wastewater constituents like those found in hospital effluents affected the removal of both CIP and FLU, but CIP degradation is less impacted probably because of its higher reactivity with sulfate radicals. Inorganic anions altered slightly the oxidation rate, while the organic compounds commonly found in wastewaters considerably reduced the degradation efficiency. ZnO doped with Fe exhibited photoactivity higher than bare zinc oxide and a commercial $TiO_2$, especially in hospital wastewater. The Fe-ZnO supported membrane can also be re-used for several oxidation runs, making this system quite suitable for larger applications in wastewater treatment processes.

**Keywords:** antibiotics; supported catalysts; oxidation; hospital wastewater, recirculation reactor.

## Water impact statement

A recirculation reactor system was designed to remove fluoroquinolones (FQs) in hospital wastewaters. FQs containing cyclopropane/piperazine rings have shown greater reactivity with radical species, and is less impacted in multi-component wastewater systems, though natural organic matter affect considerably the degradation efficiency. This new system exhibited higher photoactivity than classical $TiO_2$ in wastewater and can be re-used for several oxidation cycles.

## 1. Introduction

Antibiotics, disinfectants, cytostatics, contrast agents, metals and other medicinal residues are present at significant concentrations in hospital wastewater.[1] Fluoroquinolones (FQs) represent the third largest group of antibiotic with an increased use in hospitals, households and veterinary.[2,3] Among FQs, flumequine (FLU) and ciprofloxacin (CIP) can be found at relatively high concentrations in environmental settings. For instance, FLU can be detected at 6.9 μg $g^{-1}$ in soil and from 2.5 to 50 ng $L^{-1}$ in aquatic environments.[4,5] CIP concentration in treated hospital wastewater was found higher (~16 μg $L^{-1}$) than in environmental systems (0.6 μg $L^{-1}$).[6–8] Although these compounds often co-exist with other inorganic and organic compounds, most of previous works have mainly focused on removal processes in mono-component systems, and in pure water or synthetic contaminated waters.[9]

In order to remove antibiotics from wastewaters, advanced oxidation processes has attracted great attention through generation of reactive oxygen species (ROS).[9–11] Among these processes, photocatalysis has been widely used in order to remove organic compounds in contaminated waters. This process involves irradiation of semiconductor such as $TiO_2$ or ZnO, and when energy photons are greater than the width of semiconductor gap band, electronic gaps (commonly called holes and noted $h^+$ and electron overload noted $e^-$) are created.[11–18] These charges migrate to the surface, act as electron donors or electron acceptors and initiate the redox reactions, generating radical species.[12] ZnO is considered as an environmentally friendly catalyst due to its non-toxic nature coupled with low cost.[19] For $TiO_2$ or ZnO, the photocatalytic activity is, however, still suffering from lower quantum efficiency because of very fast recombination of photogenerated electron/hole pairs. To address this issue, incorporation of metallic (e.g. Fe) [20,21] and non-metallic species[22] have been proposed in order to enhance the photocatalytic activity. Although some studies were dedicated to the use of Fe-ZnO in decontamination reactions,[20,21] much remains to be learned on the ability of this material to

effectively remove contaminant mixture and in real wastewaters. Indeed, very few investigations have been conducted to develop cost-effective methods for the elimination of antibiotics in multi-component systems, and much less in real wastewaters where target contaminants are found with many other colloidal or dissolved substances. Furthermore, supporting these reactive phases on materials such as membrane filters may offer great advantages for high-scale applications, especially in continuous wastewater treatment pilot.[23–25]

In this study, the ability of iron doped-zinc oxide (Fe-ZnO) supported on cellulose acetate (CA) membrane to effectively remove two FQs, FLU and CIP, separately and in mixture was investigated under UV-A irradiation. Different water matrices [i.e., ultra-pure water (UPW), synthetic wastewater (SWW) and real hospital wastewater (RHW)] were used in order to test the impact of wastewater constituents on the removal performance. The CA membrane filter was selected as a support material because it is flexible, cheap and chemically stable in water. Fe-ZnO catalysts were characterized using high resolution-field emission scanning electron microscopy with energy dispersive X-ray (HR-FESEM-EDX), and X-ray diffraction (XRD). The effect of addition of oxidants such as hydrogen peroxide ($H_2O_2$), persulfate ion ($S_2O_8^{2-}$) on the removal kinetics of FLU and CIP was also investigated. Quenching experiments were conducted to identify the main reactive species in the investigated system. The reusability of iron doped-zinc oxide (Fe-ZnO) has been evaluated in successive oxidation cycles, and compared with a commercial $TiO_2$ under the same operational conditions.

## 2. Material and methods

### 2.1. Chemicals

Flumequine ($C_{14}H_{12}FNO_3$, purity > 98%), Ciprofloxacin ($C_{17}H_{18}FN_3O_3$, purity > 98%), zinc acetate dihydrate (Zn $(CH_3COO)_2{\cdot}2H_2O$, purity > 99%), iron (III) nitrate nonahydrate ($Fe(NO_3)_3$ $9H_2O$, purity > 99.95 %), absolute ethanol ($C_2H_5OH$, 100%), iso-propanol (i-PrOH,

$C_3H_8O$), *tert*-butanol (t-BuOH, $C_4H_{10}O$), potassium iodide (KI), sodium persulfate ($Na_2S_2O_8$), sodium chloride (NaCl), disodium phosphate ($Na_2HPO_4$), citric acid ($C_6H_8O_7$), ascorbic acid ($C_6H_8O_6$) and sucrose ($C_{12}H_{22}O_{11}$) were purchased from the Sigma–Aldrich chemical company. The standard Leonardite Humic acid (LHA) was provided by International Humic Substances Society (IHSS), hydrogen peroxide (35%, v/v), NaOH and HCl (37% extra pure) were provided from Acros Organics. Standard solutions were prepared with high-purity water obtained from a Millipore Milli-Q system with 18.2 MΩ cm resistivity. A cellulose support impregnated with $TiO_2$ (5 to 10 nm) made Ahlstrom company was used.

## 2.2. Preparation and characterization of Fe-ZnO supported on CA membrane

Solvothermal method was used to synthesize Fe-ZnO nanoparticles following a modified procedure of Jia et al. (2009).[26] Briefly, 0.86 g of zinc acetate dihydrate and different amount (0–1.4 % wt) of iron (III) nitrate nonahydrate was added to ethanol (60 mL) under vigorous stirring for 2 h at room temperature. At the same time, 2.4 g of NaOH was dissolved into 100 mL ethanol, and then the prepared Fe-Zn solution was added into NaOH-ethanol solution by dropwise under constant stirring for 1 h. The mixed solution was transferred to Teflon-lined autoclave and thermo-treated for 20 h at 150 °C. The dried sample was collected by centrifugation and washed several times with water and ethanol. Finally, washed particles were dried for 15 h at 60°C and only Fe-ZnO nanoparticles were calcined for 2 h at 500 °C.

In order to support Fe-ZnO nanoparticles on CA membrane filter, we followed the method previously reported in Zhao et al. (2016).[27] Different amounts of Fe-ZnO nanoparticles were dispersed in 100 mL ultra-pure water under ultra-sonication. Then, the suspension was filtered on a piece of CA membrane (64 mm in diameter and 0.45 μm in pore size). Lastly, the membrane was pressed under nitrogen gas of 0.3 MPa for 1 h and the Fe-ZnO/CA membrane was dried for 24 h at room temperature.

The morphology and particle size of synthesized Fe-ZnO were identified by HR-FESEM (SU8010, Hitachi High Technologies Corporation) equipped with EDX. The mineral phases in Fe-ZnO were analyzed with XRD (JP/MAX-3C, Rigaku) in the range of 2-theta 10–90° at a scan speed of 2°/min.

### 2.3. Recirculation reactor and degradation experiments

The degradation of FQs using ZnO and Fe-ZnO was investigated using a recirculation glass reactor described in Fig. S1‡. A peristaltic pump (Easy-Load Masterflex Head XX80 ELO 05) was used to circulate the contaminated solutions or wastewaters into the photoreactor continuously at a constant flow rate (222 mL $min^{-1}$). A UV-A lamp (PL-S 9W/10/2P; Philips, 9 W) was used as a light source at intensity of 3.4 mW $cm^{-2}$ measured by Radiometer (VLX- 3W equipped with a sensor CX 365, ALYS Technologies, Switzerland). All photocatalytic experiments were performed under similar conditions at ambient temperature and initial pH 7.0 ± 0.2. The pH value determined at the end of the reactions showed a pH around 6.9±0.3. Total 1 L of a 5 µM FLU and/or CIP solutions reacted with CA supported photocatalyst for 12 h in the dark condition to achieve the adsorption–desorption equilibrium prior to the photoreaction, then they were later exposed to UV irradiation for decontamination. At each time interval, 1.5 mL of treated solution was collected to determine the concentration of each compound by high performance liquid chromatography (HPLC). In order to investigate the effect of water matrices for photo-oxidation of FLU and CIP, we prepared a synthetic wastewater as previously described. [28] A real hospital wastewater sample was provided by the University Hospital Center of Rennes (Rennes city, France).

FLU and CIP concentrations were measured using an Alliance UV controller HPLC system equipped with an auto-sampler (Waters 717 plus), a C18 column (250 mm×4.6 mm i.d., 5 µm) and a UV detector (246 nm for FLU or 275 nm for CIP, Alliance UV 2489). The mobile phase

was a mixture of water/acetonitrile (55:45 v/v and 15:85 v/v for FLU and CIP respectively) containing 0.1% of formic acid. The flow rate of the mobile phase was set at 1 mL $min^{-1}$ in an isocratic mode. Total organic carbon (TOC) was determined using a TOC-meter (Shimadzu TOC-VCSH). All experiments of kinetic reactions were conducted in triplicates and showed a good reproducibility within 5% of relative standard deviation.

## 3. Results and discussion

### 3.1. Characterization of Fe-ZnO supported materials and UV-assisted oxidation tests

XRD patterns showed that the crystallographic structure of Fe-ZnO (0.7 wt % Fe) correspond to that of ZnO with no apparent iron oxides detected, probably due to the low detection limit of XRD measurement (needed > 2 wt. %) (Fig. 1). However, SEM images showed the effect of Fe on particle size and morphology of ZnO. Indeed, pure ZnO was nanowire in shape with 30-40 nm in diameter (Fig. 2a), while the presence of Fe caused a decrease of particle length but also a modification of morphology, *i.e.* rectangular shape nanoparticles (Fig. 2b). Incorporation of $Fe^{3+}$ ions into ZnO lattice may suppress crystal growth leading to a decrease in particle size.[29] We also observed a successful deposition of Fe-ZnO nanoparticles on CA membrane (Fig. 2b). Furthermore, the EDX analysis clearly showed the presence of Zn, Fe, O and their homogeneous distribution on CA membrane (Fig. S2‡ and Table S1‡).

The ability of different samples of Fe-ZnO (0, 0.07, 0.14, 0.28 and 0.7 wt % Fe) to remove FLU was then tested under UV-A irradiation. Generally, the degradation kinetics of organic compounds by reactive species is typically described by a second-order reaction:

$$\frac{d[Flu]}{dt} = -k[FLU][ROS] \quad (1)$$

where [ROS] is steady-state concentration of actives species, [FLU] is concentration of FLU in water, $k$ is the second-order rate constant, and $t$ is the reaction time. By assuming that concentration of actives species was constant, the degradation kinetics of FLU can be described by the pseudo-first-order equation:

$$[FLU](t) = [FLU]_0 \exp^{-k_{app}.t} \quad (2)$$

Where $k_{app}$ is obtained by linear regression of ln ($C_t/C_o$) versus time $t$.

The kinetic rate constant as well as the degradation efficiency increased with Fe content increased (Fig. 3a). It is worth noting that the initial rate constant calculated over the first stage of reaction (i.e., 5 h) is very close to the rate constant calculated over the entire reaction time, thereby supporting that the ROS concentration can be assumed constant for the entire duration of experiment (i.e. confirming the validity of eq. 2).

65% of FLU removal ($k_{app}$ = 0.042 $h^{-1}$) extent was observed in the absence of Fe (i.e., ZnO alone) indicating an activation of the semiconductor by UV-A light. Additional tests showed that removal of FLU by adsorption to supported solids is negligible. The direct photolysis of FLU under UV-A was less than 8% in 24 h ($k_{app}$ = 0.004 $h^{-1}$, Fig. S3‡). Increase in Fe content to 0.7 wt % enhanced the FLU removal up to 80% ($k_{app}$ = 0.063 $h^{-1}$) after 24 h of reaction time. However, increasing the catalyst density from 7.77 to 15.54 g $m^{-2}$/CA membrane with a constant Fe content (0.7 wt %), has no significant effect on the kinetic behavior (Fig S4‡). Since the membrane surface is likely fully covered at 7.77 g $m^{-2}$, further increase in catalyst loading would form a multilayer-like aggregation on CA membrane, and therefore the amount of surface that is subject for irradiation remains unchanged in the recirculation reactor system. The increase in Fe-ZnO activity under irradiation could be explained by the redox chemistry of

iron and the high production of reactive oxygen species. Indeed, Fe acts as a trap for the photogenerated charges, thereby preventing the electrons/holes recombination[20,30] through one or combination of two mechanisms : (i) $Fe^{3+}$ ion can react with the photogenerated electrons and be reduced to $Fe^{2+}$ which subsequently reacts with the oxygen adsorbed on the semiconductor surface to generate superoxide anion radical ($O_2^{\bullet-}$); (ii) $Fe^{3+}$ ion could also react with hole, resulting in formation of high valence iron (e.g. $Fe^{4+}$), which attacks directly the target compounds or combines with the surface hydroxyl groups to produce the $^{\bullet}OH$ radicals. The involvement of hole and hydroxyl radicals in the FLU removal was confirmed here using quenching experiments as previously described.[16,19,21]

Higher Fe content (i.e. > 0.7 wt %) inhibited the degradation process (data not shown), which can be attributed to an increase in electron/hole recombination because of modification of crystallinity and surface properties of catalysts.[20,31]

### 3.2. Impact of oxidant addition in single and binary systems

The addition of oxidant [hydrogen peroxide ($H_2O_2$) or persulfate (PS)] to the reactor system allowed faster removal kinetics (Fig.3b). Kinetic rate constants first increased with increasing $H_2O_2$ concentration and then decreased at higher oxidant dose. This typical behavior can be explained by the scavenging effect of reactive species by an excess amount of $H_2O_2$ ($k_{H_2O_2,\bullet OH}$ = $2.0\times10^7$ $M^{-1}$ $s^{-1}$,[32]). PS showed higher degradation rate constants, which continuously increased with increasing PS concentration ($k_{app}$ = 0.184 $h^{-1}$ at 0.5 mM PS). This great removal efficiency is probably due to the chemical activation of PS and generation of sulfate radicals. Formation of the latter species ($SO_4^{\bullet-}$) was confirmed here using iso-propanol ($k_{i-PrOH,\bullet OH}$ = $1.9\times10^9$ $M^{-1}$ $s^{-1}$ and $k_{i-PrOH,SO_4^{\bullet-}}$ = 4-$7.42\times10^7$ $M^{-1}$ $s^{-1}$) [32,33] and t-butanol ($k_{t-BuOH,\bullet OH}$ = $6.0\times10^8$ $M^{-1}$ $s^{-1}$, $k_{t-BuOH,SO_4^{\bullet-}}$ = 4-$8.4\times10^5$ $M^{-1}$ $s^{-1}$),[32,34] as specific scavengers in quenching experiments.[35–37]

Furthermore, the most involved radical species seem to form at the surface of solid, since addition of KI (known to react with surface bound radicals) [38,39] completely inhibited the FLU removal in the Fe-ZnO/PS/UVA system (data not shown). Photochemical activation of oxidants without Fe-ZnO (i.e., 0.5 mM PS and 0.2 mM $H_2O_2$) showed lower kinetic rate constants (0.074 $h^{-1}$ and 0.005 $h^{-1}$) (Fig. S3‡).

Higher kinetic rate constants were observed for CIP than FLU (Fig. 4a), probably due to its strong reactivity with sulfate radicals ($k_{CIP,SO_4^{\bullet-}}$= $1.2\times10^9$ $M^{-1}$ $s^{-1}$ [40]). Compounds containing cyclopropane and piperazine rings (e.g. CIP) have shown greater reactivity with radical species because the cleavage of the cyclopropane moiety via loss of one or two $CH_2$ units and the presence of piperazine ring containing two amine-N in which the lone pair electrons is conducive to a strong reaction with $SO_4^{\bullet-}$.[41,42] Compared to the single system, 1.5- and 1.8-fold decreases in degradation rate constant were observed for CIP and FLU in the mixture system (Fig. 4b), respectively, due probably to the competition effects of compounds towards reactive species.

### 3.3. Effect of water matrices

Removal kinetics of FLU or CIP in different water matrices (UPW, SWW, RHW) (See Table S2‡ for composition) were investigated under the optimal experimental condition (i.e., 0.5 mM of PS, [Fe-ZnO] = 7.77 g $m^{-2}$ membrane). Significant inhibition of FLU degradation in SWW and RHW was observed, while degradation of CIP was reduced only in RHW (Fig. S5‡). Indeed, less than 7-fold decrease in $k_{app}$ value was observed for FLU (0.184 $h^{-1}$ (UPW) to 0.025 $h^{-1}$ and 0.027 $h^{-1}$ in SWW and RHW, respectively), while less than 2-fold decrease was observed for CIP (UPW (0.943 $h^{-1}$), SWW (0.979 $h^{-1}$) and RHW (0.456 $h^{-1}$) (Fig. 5a). Similar degradation behavior was observed for FLU and CIP in the binary system (Fig. S6‡) where $k_{app}$ values decreased in RHW (Fig. 5b), probably due to competition and/or scavenging effects of

wastewater components. To address this issue, the competitive effects of organic and inorganic compounds commonly found in wastewater were tested in the Fe-ZnO/PS/UVA system. A significant inhibitive effect of organic compounds (i.e., sucrose, acetic acid, citric acid and LHA) was observed, while inorganic species showed lesser impact on the FLU degradation (Fig. 6). Indeed, the inorganic compounds (i.e., phosphate, nitrate, sulfate, and chloride) have lower kinetic rate constants with sulfate and hydroxyl radicals at neutral pH ($k_{SO_4^{\bullet-},HPO_4^{2-}}$ = 1.2 × $10^6$ $M^{-1}$ $s^{-1}$,[33] $k_{OH^{\bullet},HPO_4^{2-}}$ = 1.5 × $10^5$ $M^{-1}$ $s^{-1}$,[32] $k_{SO_4^{\bullet-},NO_3^-}$ = 2.1 × $10^6$ $M^{-1}$ $s^{-1}$,[43] $k_{SO_4^{\bullet-},Cl^-}$ = 3.0 × $10^8$ $M^{-1}$ $s^{-1}$,[44] $k_{OH^{\bullet},Cl^-}$ = 4.3 × $10^9$ $M^{-1}$ $s^{-1}$,[45]) in comparison with organic anions at the same pH ($k_{OH^{\bullet},AH^-}$ = 1.2±0.1 × $10^{10}$ $M^{-1}$ $s^{-1}$,[32] $k_{OH^{\bullet},Sucrose}$ = 2.3 × $10^9$ $M^{-1}$ $s^{-1}$,[32]), $AH^-$ represents ascorbate anion. Therefore, inhibition of FLU degradation observed in RHW may be likely ascribed to the presence of organic compounds (measured as 50 mg of TOC per L of RHW).

### 3.4. Reusability tests in hospital wastewater

Reusability of supported catalysts were investigated and compared with that of a conventional photocatalyst (i.e. $TiO_2$) under similar experimental conditions in hospital wastewater (Fig. 7). The same mass of Fe-ZnO and $TiO_2$ was used, though $TiO_2$ has much higher surface area than Fe-ZnO (300 *vs* 15 $m^2$ $g^{-1}$). In contrast to Fe-ZnO, activity of $TiO_2$ decreased significantly from the second cycle test. This strong inhibition in $TiO_2$ photoactivity could be probably due to the presence of organic and inorganic compounds in hospital wastewater which can affect the (photo) chemical mechanisms on $TiO_2$ surfaces.

As an attempt to assess the impact of these ligands, two experimental series were performed in pure water containing the most common wastewater components. First, adsorption experiments of inorganic ligands ([Phosphate] $_0$= 150 mg $L^{-1}$, [Nitrate] $_0$= 10 mg $L^{-1}$, [Sulfate] $_0$= 120 mg $L^{-1}$ and [Chloride] $_0$=250 mg $L^{-1}$) were performed in the same reactor under dark and no-oxidative conditions. The results revealed higher adsorbed amounts (expressed in mg of ligand per g of

solid) of inorganic anions onto $TiO_2$ than Fe-ZnO (Fig. S7‡). In the same way, the adsorbed amount of organic matter on $TiO_2$ (153 mgC of LHA per g of solid) was ~ 6 times higher than on Fe-ZnO (26 mgC/g). When normalized to surface area of solids, the opposite trend can be, however, observed. At neutral pH, $TiO_2$ surface is positively charged (point of zero charge pH = 6.20),[46] and thus able to sorb effectively anionic ligands species.[9] In case of FLU ($pKa$ = 6.5), more FLU adsorption to $TiO_2$ results in better photocatalytic activity ($k_{app}$ = 0.264 $h^{-1}$) compared to Fe-ZnO (Fig. 8).

In a second experimental series, removal rate constants of FLU were determined in presence of inorganic species and LHA separately at a concentration corresponding to that measured in hospital wastewater (Fig. 8). For both catalysts, the pseudo-first order rate constant decreased in presence of organic or inorganic compounds, but this fall is more pronounced in case of $TiO_2$, and particularly in presence of LHA. Indeed, kinetic rate constant decreases from $k_{app}$ = 0.264 $h^{-1}$ to $k_{app}$ = 0.015 $h^{-1}$ in presence of LHA (40 mgC $L^{-1}$). LHA possesses a high oxidation state and high aromaticity, and contains oxygenated polycyclic aromatics and carboxylic compounds which have greater affinity to metal oxides.[47–49] The binding of LHA compounds to metal-oxides may poison the catalyst surface and/or scavenge radical species.[9,50]

The dissolved iron concentration measured in solution at the end of oxidation run showed a very low release of Fe from Fe-ZnO (i.e. < 0.1 μM). In addition, XRD diffractogram recorded at the end of oxidation reaction was found to be quite similar with that recorded before reaction (Fig. 1). The stability of the catalytic activity of Fe-ZnO confirmed through reusability tests in successive oxidation cycles, could be partially attributed to the very low iron leaching during oxidation cycles and to the structural stability of the solid.

## 4. Conclusion

We have notably demonstrated that the PS/Fe-ZnO/UV-A system can be effectively used for the removal of fluoroquinolones antibiotics in hospital wastewater, and in a new recirculation reactor system. Based on the probe and scavenging experiments, sulfate radicals were mainly involved in the heterogeneous oxidation reaction. The higher degradation rate constant of CIP relative to those of FLU could be explained by the high reactivity of $SO_4^{\bullet-}$ radical with cyclopropane ring. Kinetic rate constants were found lower in binary systems with respect to those of individual compounds. The most common inorganic anions found in wastewaters can reduce the degradation efficiency, but they have much less impact compared to the organic compounds. The organic ligands and natural organic matter exhibited strong inhibition effects on $TiO_2$ activity compared to Fe-ZnO. The Fe-ZnO system exhibited better efficiency than $TiO_2$ and especially in hospital wastewater, and can be re-used for several oxidation cycles. Without ligands or organic matter, $TiO_2$ worked much better than Fe-ZnO, but when these compounds were present, they exhibited strong inhibition effects on $TiO_2$ activity compared to Fe-ZnO. The Fe-ZnO system exhibited better efficiency than $TiO_2$ in hospital wastewater and can be re-used for several oxidation cycles. Therefore, we expect that the developed system could be efficiently applied to remove antibiotics from contaminated waters, as a suitable alternative to $TiO_2$ in wastewater treatment technologies.

**Conflicts of interest**

There are no conflicts to declare.

**Acknowledgements**

We thank the Ministère de l'Enseignement Supérieur et de la Recherche Scientifique of Ivory Coast for a Ph.D. grant. This work was supported by Campus France (PHC-STAR program) and the framework of International Cooperation Program managed by National Research Foundation of Korea (NRF-2017K1A3A1A21013653).

**Footnote**

‡ Electronic supplementary information (ESI) associated with this article can be found, in the online version.

## References


O. Frédéric and P. Yves, Pharmaceuticals in hospital wastewater: Their ecotoxicity and contribution to the environmental hazard of the effluent, *Chemosphere*, 2014, **115**, 31–39.

A. J. Watkinson, E. J. Murby, D. W. Kolpin and S. D. Costanzo, The occurrence of antibiotics in an urban watershed: From wastewater to drinking water, *Sci. Total Environ.*, 2009, **407**, 2711–2723.

S. Rodriguez-Mozaz, S. Chamorro, E. Marti, B. Huerta, M. Gros, A. Sànchez-Melsió, C. M. Borrego, D. Barceló and J. L. Balcázar, Occurrence of antibiotics and antibiotic resistance genes in hospital and urban wastewaters and their impact on the receiving river, *Water Res.*, 2015, **69**, 234–242.

F. Tamtam, F. van Oort, B. Le Bot, T. Dinh, S. Mompelat, M. Chevreuil, I. Lamy and M. Thiry, Assessing the fate of antibiotic contaminants in metal contaminated soils four years after cessation of long-term waste water irrigation, *Sci. Total Environ.*, 2011, **409**, 540–547.

F. Tamtam, F. Mercier, B. Le Bot, J. Eurin, Q. Tuc Dinh, M. Clément and M. Chevreuil, Occurrence and fate of antibiotics in the Seine River in various hydrological conditions, *Sci. Total Environ.*, 2008, **393**, 84–95.

S. Castiglioni, F. Pomati, K. Miller, B. P. Burns, E. Zuccato, D. Calamari and B. A. Neilan, Novel homologs of the multiple resistance regulator marA in antibiotic-contaminated environments, *Water Res.*, 2008, **42**, 4271–4280.

L. Kovalova, H. Siegrist, H. Singer, A. Wittmer and C. S. McArdell, Hospital Wastewater Treatment by Membrane Bioreactor: Performance and Efficiency for Organic Micropollutant Elimination, *Environ. Sci. Technol.*, 2012, **46**, 1536–1545.

I. Michael, L. Rizzo, C. S. McArdell, C. M. Manaia, C. Merlin, T. Schwartz, C. Dagot and D. Fatta-Kassinos, Urban wastewater treatment plants as hotspots for the release of antibiotics in the environment: A review, *Water Res.*, 2013, **47**, 957–995.

A. R. Lado Ribeiro, N. F. F. Moreira, G. Li Puma and A. M. T. Silva, Impact of water matrix on the removal of micropollutants by advanced oxidation technologies, *Chem. Eng. J.*, 2019, **363**, 155–173.

G. Boczkaj and A. Fernandes, Wastewater treatment by means of advanced oxidation processes at basic pH conditions: A review, *Chem. Eng. J.*, 2017, **320**, 608–633.

[11] D. B. Miklos, C. Remy, M. Jekel, K. G. Linden, J. E. Drewes and U. Hübner, Evaluation of advanced oxidation processes for water and wastewater treatment – A critical review, *Water Res.*, 2018, **139**, 118–131.

[12] S. Wacławek , V. V.T. Padil, M. Černík, Major Advances and Challenges in Heterogeneous Catalysis for Environmental Applications: A Review. *Ecol. Chem. Eng. S.* 2018, **25**, 9-34.

[13] M. Pelaez, N. T. Nolan, S. C. Pillai, M. K. Seery, P. Falaras, A. G. Kontos, P. S. M. Dunlop, J. W. J. Hamilton, J. A. Byrne, K. O'Shea, M. H. Entezari and D. D. Dionysiou, A review on the visible light active titanium dioxide photocatalysts for environmental applications, *Appl. Catal. B Environ.*, 2012, **125**, 331–349.

[14] M. N. Chong, B. Jin, C. W. K. Chow and C. Saint, Recent developments in photocatalytic water treatment technology: A review, *Water Res.*, 2010, **44**, 2997–3027.

[15] K. M. Lee, C. W. Lai, K. S. Ngai and J. C. Juan, Recent developments of zinc oxide based photocatalyst in water treatment technology: A review, *Water Res.*, 2016, **88**, 428–448.

[16] N. Daneshvar, D. Salari and A. . Khataee, Photocatalytic degradation of azo dye acid red 14 in water on ZnO as an alternative catalyst to TiO2, *J. Photochem. Photobiol. Chem.*, 2004, **162**, 317–322.

[17] S. Sakthivel, B. Neppolian, M. V. Shankar, B. Arabindoo, M. Palanichamy and V. Murugesan, Solar photocatalytic degradation of azo dye: comparison of photocatalytic efficiency of ZnO and TiO2, *Sol. Energy Mater. Sol. Cells*, 2003, **77**, 65–82.

[18] C. Gomez-Solís, J. C. Ballesteros, L. M. Torres-Martínez, I. Juárez-Ramírez, L. A. Díaz Torres, M. Elvira Zarazua-Morin and S. W. Lee, Rapid synthesis of ZnO nano-corncobs from Nital solution and its application in the photodegradation of methyl orange, *J. Photochem. Photobiol. Chem.*, 2015, **298**, 49–54.

[19] F. Sordello, I. Berruti, C. Gionco, M. C. Paganini, P. Calza and C. Minero, Photocatalytic performances of rare earth element-doped zinc oxide toward pollutant abatement in water and wastewater, *Appl. Catal. B Environ.*, 2019, **245**, 159–166.

[20] M. C. Paganini, A. Giorgini, N. P. F. Gonçalves, C. Gionco, A. Bianco Prevot and P. Calza, New insight into zinc oxide doped with iron and its exploitation to pollutants abatement, *Catal. Today*, 2019, **328**, 230–234.

[21] R. Saleh and N. F. Djaja, UV light photocatalytic degradation of organic dyes with Fe-doped ZnO nanoparticles, *Superlattices Microstruct.*, 2014, **74**, 217–233.

[22] L. Pan, T. Muhammad, L. Ma, Z.-F. Huang, S. Wang, L. Wang, J.-J. Zou and X. Zhang, MOF-derived C-doped ZnO prepared via a two-step calcination for efficient photocatalysis, *Appl. Catal. B Environ.*, 2016, **189**, 181–191.

[23] A. Rajeswari, S. Vismaiya and A. Pius, Preparation, characterization of nano ZnO-blended cellulose acetate-polyurethane membrane for photocatalytic degradation of dyes from water, *Chem. Eng. J.*, 2017, **313**, 928–937.

[24] P. S. Chauhan, R. Kant, A. Rai, A. Gupta and S. Bhattacharya, Facile synthesis of ZnO/GO nanoflowers over Si substrate for improved photocatalytic decolorization of MB dye and industrial wastewater under solar irradiation, *Mater. Sci. Semicond. Process.*, 2019, **89**, 6–17.

[25] L. Valenzuela, A. Iglesias, M. Faraldos, A. Bahamonde and R. Rosal, Antimicrobial surfaces with self-cleaning properties functionalized by photocatalytic ZnO electrosprayed coatings, *J. Hazard. Mater.*, 2019, **369**, 665–673.

[26] T. Jia, W. Wang, F. Long, Z. Fu, H. Wang and Q. Zhang, Fabrication, characterization and photocatalytic activity of La-doped ZnO nanowires, *J. Alloys Compd.*, 2009, **484**, 410–415.

[27] H. Zhao, S. Chen, X. Quan, H. Yu and H. Zhao, Integration of microfiltration and visible-light-driven photocatalysis on g-C 3 N 4 nanosheet/reduced graphene oxide membrane for enhanced water treatment, *Appl. Catal. B Environ.*, 2016, **194**, 134–140.

[28] S. Babić, M. Periša and I. Škorić, Photolytic degradation of norfloxacin, enrofloxacin and ciprofloxacin in various aqueous media, *Chemosphere*, 2013, **91**, 1635–1642.

[29] S. Sriwichai, H. Ranwongsa, K. Wetchakun, S. Phanichphant and N. Wetchakun, Effect of iron loading on the photocatalytic performance of Bi2WO6 photocatalyst, *Superlattices Microstruct.*, 2014, **76**, 362–375.

[30] M. M. Ba-Abbad, A. A. H. Kadhum, A. B. Mohamad, M. S. Takriff and K. Sopian, Visible light photocatalytic activity of Fe3+-doped ZnO nanoparticle prepared via sol–gel technique, *Chemosphere*, 2013, **91**, 1604–1611.

[31] Priyanka and V. C. Srivastava, Photocatalytic Oxidation of Dye Bearing Wastewater by Iron Doped Zinc Oxide, *Ind. Eng. Chem. Res.*, 2013, **52**, 17790–17799.

[32] G. V. Buxton, C. L. Greenstock, W. P. Helman and A. B. Ross, Critical Review of rate constants for reactions of hydrated electrons, hydrogen atoms and hydroxyl radicals (·OH/·O$^-$ in Aqueous Solution, *J. Phys. Chem. Ref. Data*, 1988, **17**, 513–886.

P. Neta, R. E. Huie and A. B. Ross, Rate Constants for Reactions of Inorganic Radicals in Aqueous Solution, *J. Phys. Chem. Ref. Data*, 1988, **17**, 1027–1284.

M. Anbar and P. Neta, A compilation of specific bimolecular rate constants for the reactions of hydrated electrons, hydrogen atoms and hydroxyl radicals with inorganic and organic compounds in aqueous solution, *Int. J. Appl. Radiat. Isot.*, 1967, **18**, 493–523.

Y. Wu, A. Bianco, M. Brigante, W. Dong, P. de Sainte-Claire, K. Hanna and G. Mailhot, Sulfate Radical Photogeneration Using Fe-EDDS: Influence of Critical Parameters and Naturally Occurring Scavengers, *Environ. Sci. Technol.*, 2015, **49**, 14343–14349.

E. M. Rodríguez, G. Márquez, M. Tena, P. M. Álvarez and F. J. Beltrán, Determination of main species involved in the first steps of TiO2 photocatalytic degradation of organics with the use of scavengers: The case of ofloxacin, *Appl. Catal. B Environ.*, 2015, **178**, 44–53.

M. Kamagate, A. Amin Assadi, T. Kone, L. Coulibaly and K. Hanna, Activation of persulfate by irradiated laterite for removal of fluoroquinolones in multi-component systems, *J. Hazard. Mater.*, 2018, **346**, 159–166.

S. T. Martin, A. T. Lee and M. R. Hoffmann, Chemical mechanism of inorganic oxidants in the TiO2/UV process: increased rates of degradation of chlorinated hydrocarbons, *Environ. Sci. Technol.*, 1995, **29**, 2567–2573.

L. Xu and J. Wang, Magnetic Nanoscaled Fe3O4/CeO2 Composite as an Efficient Fenton-Like Heterogeneous Catalyst for Degradation of 4-Chlorophenol, *Environ. Sci. Technol.*, 2012, **46**, 10145–10153.

M. Mahdi-Ahmed and S. Chiron, Ciprofloxacin oxidation by UV-C activated peroxymonosulfate in wastewater, *J. Hazard. Mater.*, 2014, **265**, 41–46.

C. Jiang, Y. Ji, Y. Shi, J. Chen and T. Cai, Sulfate radical-based oxidation of fluoroquinolone antibiotics: Kinetics, mechanisms and effects of natural water matrices, *Water Res.*, 2016, **106**, 507–517.

H. Guo, T. Ke, N. Gao, Y. Liu and X. Cheng, Enhanced degradation of aqueous norfloxacin and enrofloxacin by UV-activated persulfate: Kinetics, pathways and deactivation, *Chem. Eng. J.*, 2017, **316**, 471–480.

H. Gao, J. Chen, Y. Zhang and X. Zhou, Sulfate radicals induced degradation of Triclosan in thermally activated persulfate system, *Chem. Eng. J.*, 2016, **306**, 522–530.

Y. Yang, J. J. Pignatello, J. Ma and W. A. Mitch, Comparison of Halide Impacts on the Efficiency of Contaminant Degradation by Sulfate and Hydroxyl Radical-Based Advanced Oxidation Processes (AOPs), *Environ. Sci. Technol.*, 2014, **48**, 2344–2351.

S. Khan, X. He, J. A. Khan, H. M. Khan, D. L. Boccelli and D. D. Dionysiou, Kinetics and mechanism of sulfate radical- and hydroxyl radical-induced degradation of highly chlorinated pesticide lindane in UV/peroxymonosulfate system, *Chem. Eng. J.*, 2017, **318**, 135–142.

A. A. Dougna, B. Gombert, T. Kodom, G. Djaneye-Boundjou, S. O. B. Boukari, N. K. V. Leitner and L. M. Bawa, Photocatalytic removal of phenol using titanium dioxide deposited on different substrates: Effect of inorganic oxidants, *J. Photochem. Photobiol. Chem.*, 2015, **305**, 67–77.

K. Yang, D. Lin and B. Xing, Interactions of Humic Acid with Nanosized Inorganic Oxides, *Langmuir*, 2009, **25**, 3571–3576.

H. Kerndorff and M. Schnitzer, Sorption of metals on humic acid, *Geochim. Cosmochim. Acta*, 1980, **44**, 1701–1708.

S. Jayalath, H. Wu, S. C. Larsen and V. H. Grassian, Surface Adsorption of Suwannee River Humic Acid on $TiO_2$ Nanoparticles: A Study of pH and Particle Size, *Langmuir*, 2018, **34**, 3136–3145.

M. Drosos, M. Ren and F. H. Frimmel, The effect of NOM to $TiO_2$ : interactions and photocatalytic behavior, *Appl. Catal. B Environ.*, 2015, **165**, 328–334.

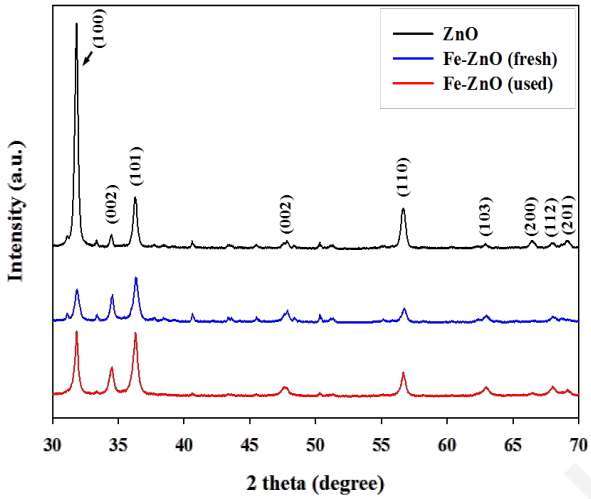


**Fig. 1**. X-Ray Diffractograms of ZnO and 0.7 wt % Fe-ZnO before and after five consecutive oxidation runs in hospital wastewater.

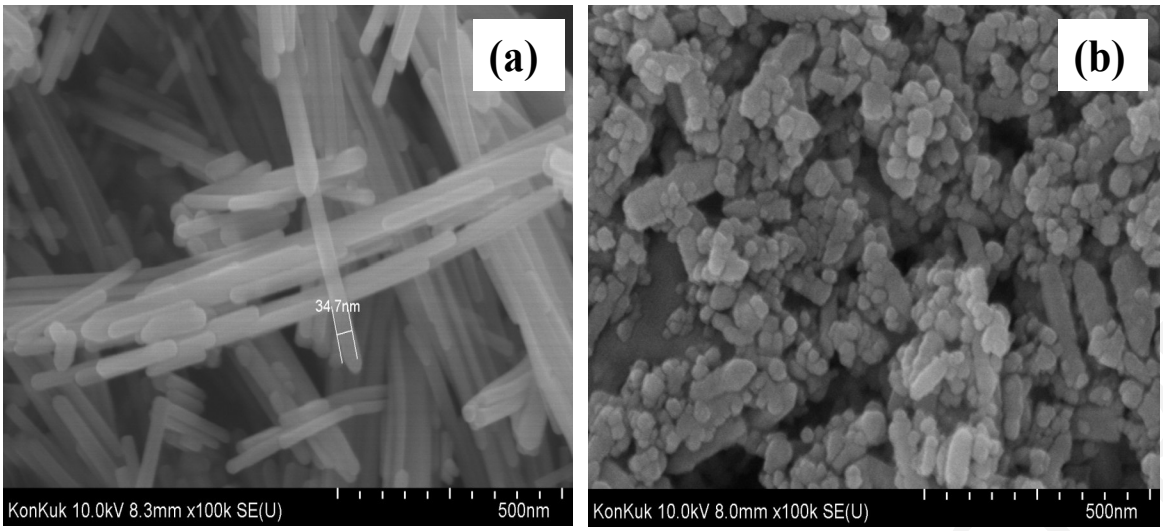


**Fig. 2**. HR-FESEM images of (a): ZnO/CA membrane and (b): Fe-ZnO (0.7 wt % Fe)/CA membrane. Abbreviations: high resolution-field emission scanning electron microscopy with energy dispersive X-ray (HR-FESEM-EDX).

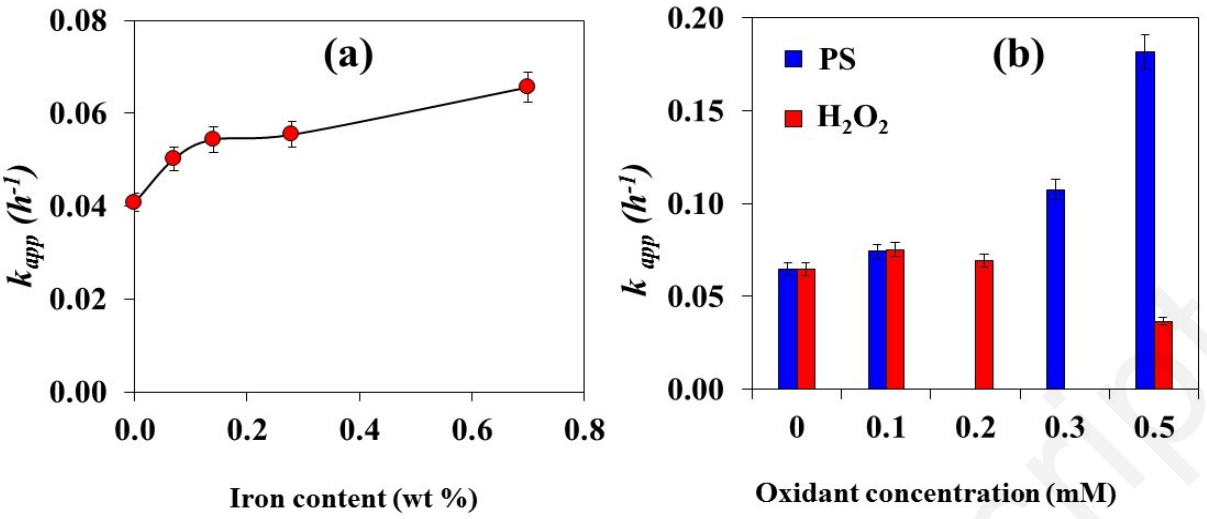


530

531**Fig. 3**. Kinetic rate constants, $k_{app}$ of FLU removal as a function of (a) Fe loading on ZnO
532supported catalyst and (b) oxidant concentration using 0.7 wt % Fe-ZnO catalyst. Experimental
533conditions: $[FLU]_0$ = 5 µM, [catalyst] = 7.77 g $m^{-2}$ on CA membrane, UV-A reaction time = 24
534h, $pH_0$ = 7.0 ± 0.2, V = 1 L, recirculation flow rate = 222 mL $min^{-1}$ (the correlation coefficients
535were more than 0.99 for all experiments). Abbreviations: FLU = flumequine, PS = Persulfate,
536$H_2O_2$ = hydrogen peroxide.

537

538

539

540

541

542

543

544

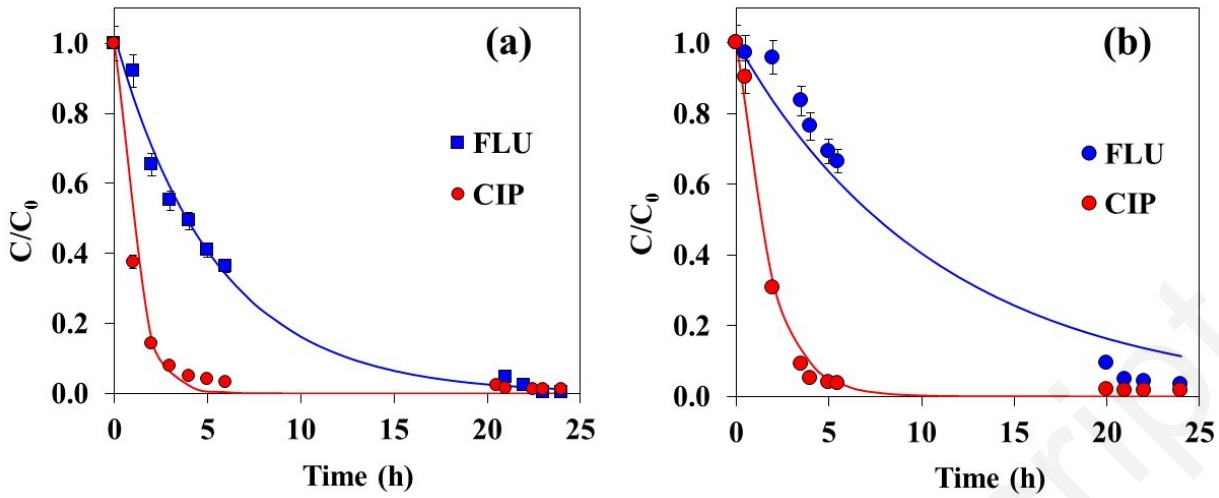


545

546**Fig. 4**. Degradation kinetics of FLU and CIP in single (a) and binary (b) systems under UV-A
547irradiation. Experimental conditions: [FLU] $_0$ = 5 µM, [0.7 wt % Fe-ZnO] = 7.77 g $m^{-2}$ CA
548membrane, UV-A reaction time = 24 h , pH $_0$ = 7.0 ± 0.2, V = 1 L, recirculation flow rate = 222
549ml $min^{-1}$. The correlation coefficients for kinetic model are more than 0.98 for all experiments.
550Abbreviations: FLU = flumequine, CIP = ciprofloxacin, PS = persulfate.

551

552

553

554

555

556

557

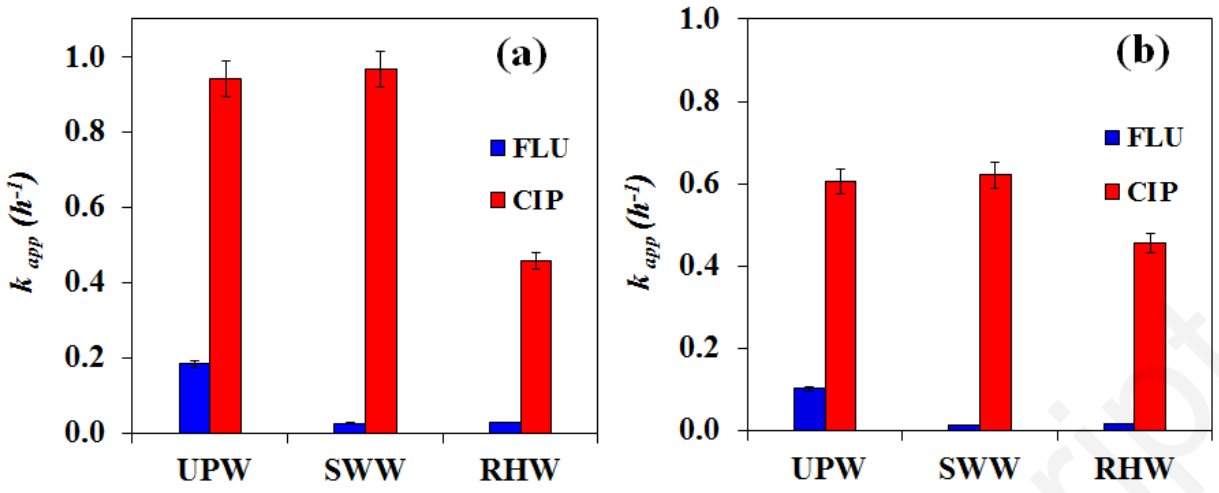


**Fig. 5**. Kinetic rate constants of FLU and CIP degradation obtained in different water matrices in (a) single and (b) binary systems. Experimental conditions: $[FLU]_0 = [CIP]_0 = 5$ µM, [Fe-ZnO] = 7.77 g $m^{-2}$ CA membrane, $[PS]_0 = 0.5$ mM, UV-A reaction time = 24 h for CIP and FLU in UPW and 72 h for FLU in SWW and RHW, $pH_0 = 7.0 \pm 0.2$, V = 1 L, recirculation flow rate = 222 mL $min^{-1}$ (the correlation coefficients were more than 0.99 for all experiments). Abbreviations: FLU = flumequine and CIP = ciprofloxacin, PS = persulfate, UPW = Ultra-pure water, SWW = Synthetic wastewater, RHW = Real hospital wastewater.

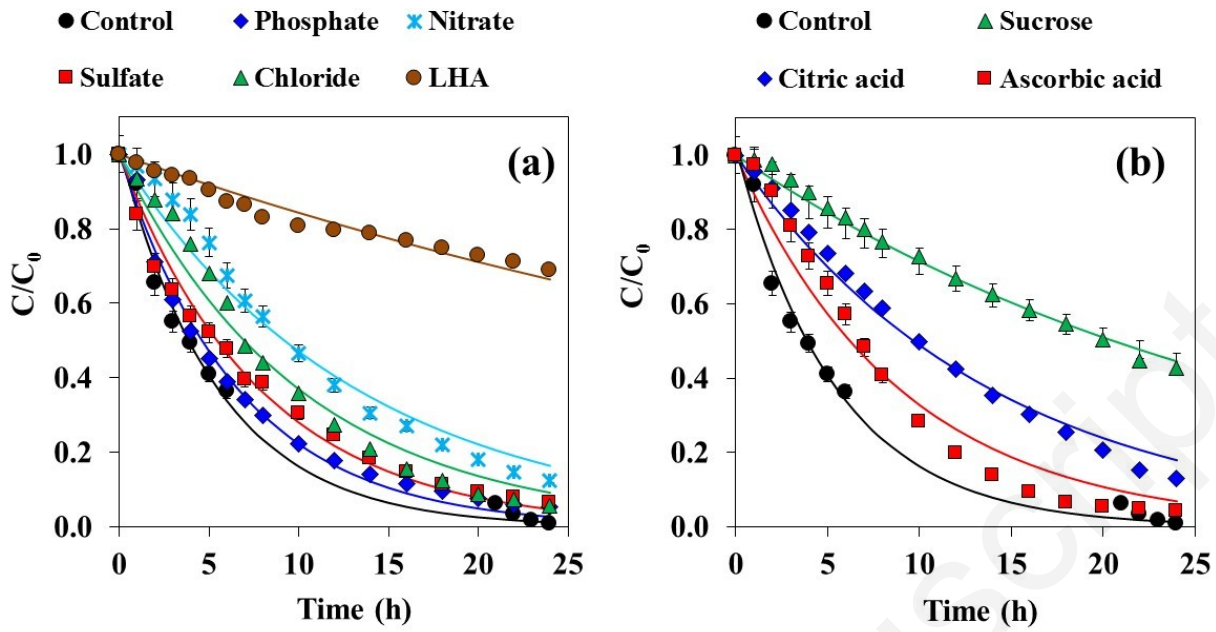


574

575

576**Fig. 6**: Effect of inorganic ions and LHA (a) and organic ligands (b) on FLU removal using 0.7
577wt % Fe-ZnO. Experimental conditions: [FLU] $_0$ = 5µM, [PS] $_0$ = 0.5mM, pH$_0$ = 7.0 ± 0.2, [Fe-
578ZnO] = 7.77 g m$^{-2}$ CA membrane, [Phosphate] $_0$ = 150 mg L$^{-1}$, [Nitrate] $_0$ = 10 mg L$^{-1}$, [Sulfate] $_0$
579= 120 mg L$^{-1}$, [Chloride] $_0$ =250 mg L$^{-1}$ , [LHA] $_0$ = 40 mgC L$^{-1}$, [Ascorbic acid] $_0$ = 30 mg L$^{-1}$,
580[Citric acid] $_0$ = 50 mg L$^{-1}$, [Sucrose] $_0$ = 100 mg L$^{-1}$, reaction time = 24 h, V = 1 L, mass of
581catalyst = 0.025 g, recirculation flow rate = 222 mL min$^{-1}$. The correlation coefficients were
582more than 0.98 for all experiments. Abbreviation: FLU = flumequine, PS = persulfate, LHA =
583Leonardite Humic Acid.

584

585

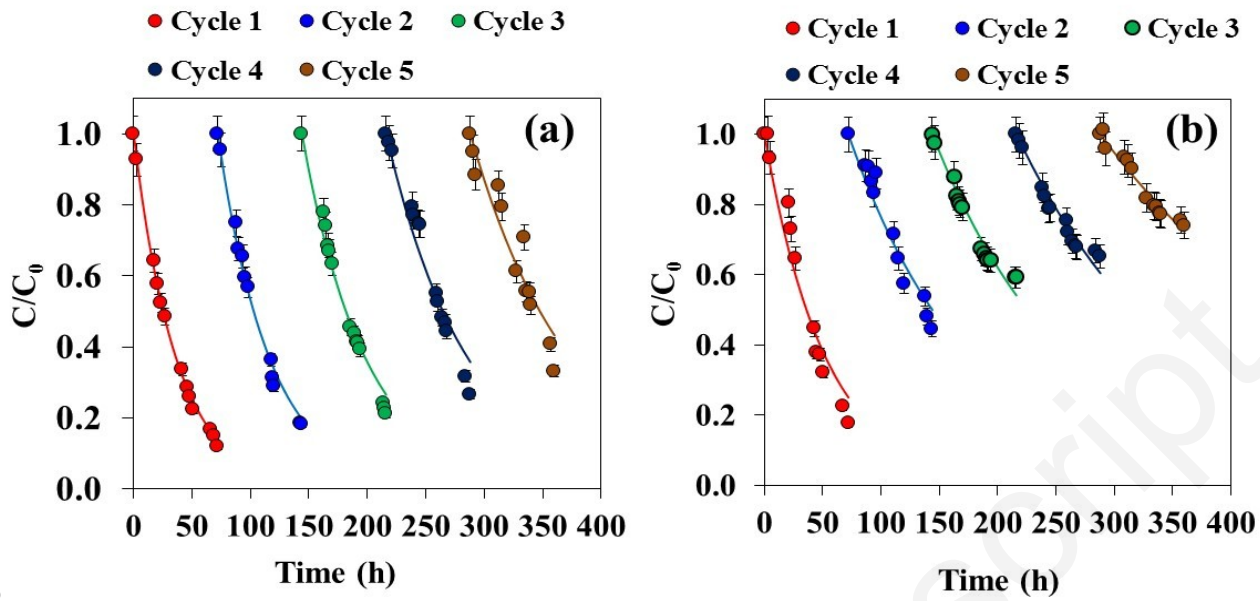


586

587**Fig. 7.** Reusability cycles of Fe-ZnO in hospital wastewater. (a): 0.7 wt % Fe-ZnO and (b): 588$TiO_2$. Experimental conditions: $[FLU]_0$ = 5 µM, $[PS]_0$ = 0.5 mM, mass of catalyst = 0.025 g, 589UV-A reaction time = 72 h, $pH_0$ = 7.0 ± 0.2, V = 1 L, recirculation flow rate = 222 mL $min^{-1}$. 590The correlation coefficients were more than 0.98 for all experiments. Abbreviations: FLU = 591flumequine, PS = Persulfate

592

593

594

595

596

597

598

599

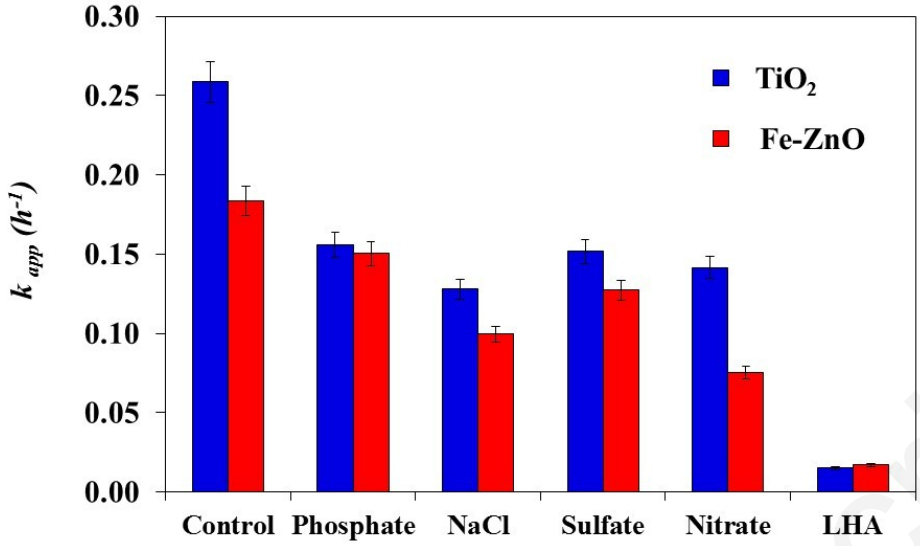


**Fig. 8**: Effect of humic acids and inorganic ligands on removal kinetics using 0.7 wt % Fe-ZnO or $TiO_2$ under UVA irradiation. Experimental conditions: $[FLU]_0$ = 5µM, $[PS]_0$ =0.5mM, $pH_0$ = 7.0 ± 0.2, $[Phosphate]_0$ = 150 mg $L^{-1}$, $[Nitrate]_0$ = 10 mg $L^{-1}$, $[Sulfate]_0$ = 120 mg $L^{-1}$, $[Chloride]_0$ = 250 mg $L^{-1}$ , $[LHA]_0$ = 40 mgC $L^{-1}$, reaction time = 24 h, V = 1 L, catalyst mass = 0.025 g, recirculation flow rate = 222 mL $min^{-1}$. Abbreviations: FLU = flumequine, PS = persulfate, LHA = Leonardite Humic Acid.